

Rapid Automated Measurement of Body Fat Tissue from Whole Body MRI

Darren D. Brennan¹, Paul F. Whelan², Kevin Robinson², Ovidiu Ghita², Julie M. O'Brien¹, Robert
Sadleir², Stephen J. Eustace¹

1

Department of Radiology, Cappagh National Orthopaedic
Hospital, Finglas, Dublin, 11 Ireland.
Address correspondence to S. J. Eustace.

2

Vision Systems Group, Dublin City University,
Dublin, Ireland.

Abstract

Objective The purpose of this article is to determine the feasibility of using computer assisted diagnosis (CAD) techniques to automatically identify, localize, and measure body fat tissue from a rapid whole-body MRI examination

Design Prospective investigative study.

Setting Dublin, Ireland.

Participants 42 volunteers (21 male, 21 female) aged 18 to 56. The study group consisted of healthy volunteers with a wide range of body weights, and included a cohort of high performance athletes.

Main outcome measures The provision of an automated system, which assesses subjects' whole body MRI scans and which provides numerical and visual feedback to illustrate the findings. The system generates results in a matter of minutes allowing for an initial assessment to be performed immediately following the completion of an MRI scan. By highlighting areas where body fat is concentrated the system allows radiologists to quickly identify and examine regions of interest in the scan.

Results Rapid, accurate, and reproducible delineation of body fat distribution can be obtained using whole body MRI techniques and Computer Aided Diagnosis.

Conclusions Whole-body MRI in conjunction with CAD allows a fast, automatic, and accurate approach to body fat measurement and localization and can be a useful alternative to body mass index. Whole-body fat analysis can be achieved in less than 5 min.

Introduction

The accurate determination of a person's total body fat is an important issue in medical analysis because obesity is a significant contributing factor to a variety of serious health problems. The medical literature identifies a wide range of diseases that are closely linked to obesity. Current methods of fat assessment are largely inaccurate, and most current methods of fat determination cannot show regional fat distribution, which is important in defining disease risk. We introduce a method that combines computer-aided techniques with whole-body MRI techniques and enables accurate quantification and visualization of total body fat burden and regional fat distribution. This technique may be important in identifying and treating at-risk populations

Materials and methods

Patients

This study included 42 patients (21 men and 21 women) who were recruited through local in-hospital advertising and a hospital-related sports clinic. These volunteers included a cohort of international rowers, a group of elite athletes in whom body fat estimation is of particular importance as individuals are weight restricted. Local institutional board approval was obtained. Informed consent was acquired from each subject, and his or her weight and height were recorded. These were used to calculate the body mass index (BMI) in each patient.

Full body MR acquisition

MR images were acquired on a 1.5 T imaging unit (Intera, Philips Medical Systems), which was fitted with a tabletop extender and allowed automated table movements. With the tabletop extender, caudocranial coverage of 200 cm is achieved, which allows examination of all but the tallest subjects. Images are acquired in six to seven fully integrated stacks with a small overlap. We acquired coronal

T1-weighted gradient-echo images (TR/TE,112/1.62; flip angle, 70°, number of signals averaged, 1; matrix, 256 × 256; 80% rectangular field of view, 189 × 189). Automated voxel interpolation was used to yield voxels of 2.02 × 2.02 × 8.00 mm³

For the scanning process, patients are placed supine with their hands crossed over the abdomen. This enables the subjects' upper limbs to be imaged. We had initially placed the subjects' hands by the sides but found that this caused aliasing artifact. After imaging, the raw data are transferred, in DICOM format, to a workstation for analysis. At the workstation, complex sets of algorithms are sequentially applied to each data set to isolate fat.

Analysis of DICOM images

In full-body MRI, the subject is imaged in a set of overlapping coronal sections. The resulting series of MR images must be reconstructed into a volumetric data set to facilitate analysis. There are two issues that require particular attention in this process: spatial registration and gray-scale matching. To achieve correct spatial registration, we use location and orientation vectors stored in the DICOM headers. This allows us to accurately position each image within a global coordinate system. In this way, we can account for any overlap between adjacent coronal slices and correctly generate the final volume.

Gray-scale matching is necessary because there can be significant intensity offsets between successive coronal sections due to the nature of the MRI acquisition process, particularly the close spatial relationship of the back to the receiver coils. It is necessary to minimize these effects to optimize the performance of the automated analysis procedure. We achieve this using histogram matching. An intensity histogram is constructed for each coronal section, the characteristic peak representing soft tissue is algorithmically identified in each case, and the set of peaks are aligned to match the gray-scale distributions across all sections.

Image Segmentation

A visual examination of the images contained in the data sets reveals that the fat tissues tend to have a higher gray-scale value than other tissues. But these images also indicate that there is a high gray-scale variation within the image regions representing fat tissues. Also, even after histogram matching, the gray-scale values for fat in some situations overlap those associated with other nominally lower-intensity tissues such as those representing liver or brain. Therefore, accurate segmentation cannot be achieved by applying simple methods based on thresholding. To cope with these problems, we have devised a four-step segmentation algorithm. An initial threshold level is calculated based on an analysis of the data histogram. The peak representing soft tissue is located, and voxels with values that fall above the end of this peak are initialized as potential fat voxels. We then use a boundary-enhancement step to compensate for signal drop-off in some peripheral regions of the data. Next we apply a 3D region-growing procedure. Finally, we apply a region-refining process whereby the candidate voxels are grouped into connected regions [1]. Through this process, we arrive at a robust segmentation of the signal due to fat tissue within the data volume.

Total body fat calculation

Calculation of the total body fat (TBF) is performed using the following formula:

$$TBF = (N\text{FatVoxels})(Voxel_Dim)(Fat_Density)$$

where $N\text{FatVoxels}$ is the total number of fat voxels contained in the data set, $Voxel_Dim$ is the voxel dimension (in cm^3), and $Fat_Density$ is the density of the fat tissue (in g/cm^3). The voxel dimensions can be extracted from the DICOM header and the data sets used in our study have mostly had dimensions of $2.02 \times 2.02 \times 8.00 \text{ mm}^3$. The medical literature indicates that fat tissue density can be regarded as constant [2] and is usually assigned a value of $0.9196 \text{ g}/\text{cm}^3$. The fat content is determined

by counting the fat tissue voxels contained in the segmented data (marked in yellow in Fig. 1). We normalized these values to yield the total body fat in kilograms.

Results

Basic User Functions

Analysis results are presented in a number of ways. Simple orthogonal review allows axial, coronal, and sagittal sections to be examined, highlighting regions that have been classified as body fat. Color mark-up of the images provides effective visual feedback, improving the readability of the data (Fig. 1). This form of review also allows detailed examination of the distribution of fat throughout the body and facilitates the easy identification of areas of particular fat concentration.

Three-dimensional volume-rendered views (Fig. 2) provide an excellent overview of the data, and when used with data space clipping, can effectively visualize the body fat distribution within a volume of interest, providing a more complete view and comprehensive breakdown of the distribution of fatty tissue within the body.

In addition to these visual tools, numeric results are presented to the user. Figure 3 shows an example of the typical results generated by the system. Estimates are made of the subjects' height and weight, and measurements are performed to calculate values for the actual and percentage body fat detected, measured by volume and by weight. All these calculations are performed automatically without any initialization or subsequent intervention required on the part of the user. The entire analysis process, from raw DICOM data to final results, takes less than 2 min.

A database of 42 data sets (Table 1) containing 21 men and 21 women in the age range 18–56 years was used to assess the segmentation algorithm. The BMI was calculated directly from the patients' mass and height and indirectly using the segmentation results. The directly measured BMI values of these data sets range from 18 to 35. Comparison of the direct and indirect methods was used to validate the segmentation procedure, and a good correlation was found (Fig. 4). Much of the data spread in the

graph in Figure 4 is due to incomplete body acquisitions in the MRI scanner. Restricting the data to the 21 most complete data sets, where data loss at the extremities, especially at the feet of tall subjects, is kept to a minimum, results in a far superior straight-line fit with greatly reduced deviations from the fitted line in the restricted data subsample. This is shown in the broken line and its associated subset of data points indicated in Figure 4. The sample points representing incomplete acquisitions all fall above the broken line and pull the full-sample trend line (the solid line) in an upward direction. This reflects the relative effect of the missing data on the BMI and percentage body fat calculations. The missed data represent a relatively small volume and, therefore, weight (the feet and ankles), but can result in a disproportionately large variation in the estimated height of the subject. With down-pointing toes, the change can be as much as 30 cm in some cases.

These two factors result in little difference in the estimated percentage body fat but can cause a significant elevation in the estimated BMI value since the subject is estimated to be shorter but not much lighter than would be the case were the measurements based on a complete data set. Note that in the case of complete data sets, the automatic method consistently estimates a BMI less than the measured BMI. This is due to an overestimation in the height caused by down-pointing toes. An alteration in the acquisition protocol supporting the subject's feet vertically could correct for this. Correspondingly, calculated BMIs based on incomplete data sets tend to be higher than the equivalent measured values for the reasons given. These observations support the assertion that the automatic measurements achieved represent accurate results for the data under examination. Avoiding errors in height estimation can be easily performed by supporting the feet in a neutral position and by recognizing that 200 cm is the maximum obtainable coverage. With careful technique, all but the tallest patients can be included.

The measure that is of greater interest is that of percentage body fat, the accurate determination of which was the main goal of the study. The results showed that there was a reasonable correlation between this measurement and BMI, with the expected sex differences as highlighted in Figure 5. However, the complexity of the relationship illustrated in Figure 5 confirms the recognized

shortcomings of BMI as a measurement of body fat level. The results for the cohort of international rowers highlight their unusually high muscle mass, showing one of the drawbacks of BMI—its inability to distinguish between body mass stemming from different sources. The results are presented in Table 1 and Figures 4 and 5. In all cases, results were obtained within minutes of receiving the DICOM data.

Discussion

Obesity is increasingly recognized as a major health problem in the developed world. An emotive issue that is firmly in the public eye, fat deposition is a complex process that is poorly understood. Genetic, environmental, and hormonal influences are all known to have an effect. It is known from diseases such as growth hormone deficiency and hypercortisolism, which predispose to increased fat deposition, that abnormal fat distribution often occurs in a central or visceral distribution. This visceral adiposity is a known risk factor for hypertension and cardiovascular disease [3]; cerebrovascular disease [4]; insulin resistance and type 2 diabetes [4]; endometrial, colon, and other forms of cancer [5]; and depression and other psychological dysfunctions [6–8]. Despite extensive research interest in obesity, estimation of body fat content in a noninvasive manner is difficult. Widely used anthropometric measurements are crude markers of body fat distribution and also allow no breakdown of regional distribution of fat. In addition, they are subject to extensive inter- and intraobserver error and have poor reproducibility. Many authors have questioned their validity in defined populations such as the young [9] and in different ethnic groups [10]. The derivation of body fat from anthropometric means is difficult and requires the use of equations, more than 3,000 of which have been validated in different age, sex, and ethnic populations.

The BMI, which infers body fat content from height and weight alone is convenient for mass screening, but again, its validity has been questioned in different ethnic groups and age populations [11–13]. It is also known to be inaccurate in athletic individuals [14, 15] and elderly individuals [14, 16] due to extremes of muscle content. In addition, it gives no insight into the regional distribution of fat.

Complex laboratory-based methods of total body fat measurement include techniques such as hydrodensity, radioactive dilution, and air displacement (Bod Pod, Life Measurement). While water displacement is recognized as the gold standard, it is time consuming, extremely inconvenient, and not widely available. The validity of some of these techniques has also been questioned [17–19].

More recently, new techniques have been developed, and among the most important are dual-energy X-ray absorptiometry (DEXA), near infrared interactance (NIR), and total body electrical conductivity (TOBEC). DEXA is probably the most widely available and appears to be reasonably accurate, although it does require ionizing radiation exposure. TOBEC, segmental, and total body impedance infer body fat distribution from resistance to an electric current and have their detractors [18, 20, 21]. In most cases, these techniques are accurate but the equipment is dedicated and expensive, and this is a deterring factor for their application in current medical investigations. In addition, DEXA requires exposure to ionizing radiation.

In our study, we compared our investigational method for fat analysis with BMI alone. While a broad correlation was obtained, we think that most of the disparity between the two techniques is based on a flawed reference standard. Comparison with a better method of fat analysis such as water displacement would have increased the validity of our results, but we did not have access to such techniques. Furthermore, institutional review board restrictions precluded us from using any methods that included ionizing radiation. Finally, even if we had an absolute reference method available for comparison, no gold-standard test exists today for quantifying regional fat distribution, which we think is one of the more important outcomes of our research methods.

Previous authors have used cross-sectional imaging techniques to estimate body fat content [22–24]. CT is widely available, quick, and, because of the unique reproducibility of fat attenuation, suitable for automated image analysis. However, the prohibitive dose of radiation involved precludes its use in a general population. In addition, whole-body imaging using a helical or newer generation MDCT would necessitate extensive image interpolation, thus potentially introducing bias.

MRI, although not as widely available as CT, is becoming more widely used and does not entail ionizing radiation. Previous authors have determined the accuracy and reproducibility of MRI for fat analysis when compared with cadaveric dissection [25] and in animal models [26]. On T1-weighted imaging, fat returns high signal because of a high concentration of relatively immobile protons. Only paramagnetic substances such as iron or melanin, highly viscous fluids, and moving spins (e.g., flowing blood) also return high signal using this sequence. Iron and melanin are not present in the body in any meaningful quantities. In addition, because we acquired coronal images oriented parallel to the axes of most major blood vessels, flow-related enhancement was not a major issue.

Although MRI for fat analysis has already been used by previous authors, a review of the literature reveals that a wide spectrum of techniques has been used, often consisting of single or selected slices, with subsequent extrapolation to the remainder of the body [27–30]. Other early studies on whole-body MRI for fat analysis used gaps of 1–3 cm between axial slices, which require interpolation and thus inevitably introduce bias. Indeed, previous authors have shown that subsampling and limited scanning do introduce bias and increased uncertainty into recorded fat measurements [29]. In our study, we achieved whole-body coverage without slice gaps, thus eliminating any potential for bias and ensuring accurate and reproducible results. In addition, developments in hardware, field homogeneity, and the use of gradient-echo sequences have reduced our imaging time to approximately 140 sec.

Our technique effectively divides the body into voxels of $2.02 \times 2.02 \times 8.00 \text{ mm}^3$. By dividing the body into such small 3D voxels and subsequently using computer-assisted diagnostic (CAD) techniques as outlined, a definite representation of fat distribution is obtained, and potential inaccuracies due to partial volume effects are kept to a minimum. A degree of controversy exists in the literature as to the exact biochemical consistency of the tissue detected as fat by MRI. However, most authors accept that adipose tissue is composed of 84.67% triglyceride, 12.67% water, and 2.66% protein, giving a density of 0.9196 kg/L [31]. In addition, this biochemical consistency appears to be homogeneous throughout the human body, so that confounding variables that underlie the difficulties with other body composition methods such as age, sex, and ethnic origin are removed. Thus, the use of equations, apart

from the automated total body fat calculation mentioned previously, is removed. In our cohort of patients, we examined a group with a wide spectrum of body fat levels and distributions without obvious detriment or difficulty, including athletes who are ill served by other available methods.

In this investigation, we illustrate how the use of CAD techniques based on the methodologies of advanced image processing and analysis can be used to quantify the fat distribution within the body in sequences of fullbody MR images. The outcome of this research effort is a system that assesses a subject's full-body MRI scan, providing numeric and visual feedback to illustrate its findings. This system generates results in a matter of minutes, allowing for an initial assessment to be performed immediately after the completion of an MRI scan. By highlighting areas where body fat is concentrated, the system allows radiologists to quickly identify and examine regions of interest in the scan.

The system's numeric outputs also provide an accurate measurement of body fat as a percentage of whole-body mass. This is an important metric, which is difficult and time consuming to derive by alternative means. As alluded to previously, the distribution of actual fat tissue in the body is an important measurement of health and overall fitness and is not well quantified by BMI. In this regard, the assessment of body fat in athletes involved in programs of intensive training was an area of particular importance in our study. The ability to localize fat distribution and to show an athlete exactly where it is on the body is of great interest because such information can be used to help shape the training schedule of the athlete. This has particular import for many weight-restricted athletes, such as rowers, boxers, and jockeys. The entire body is covered, without gaps, in an imaging time of approximately 2 mins 20 secs, and 32 coronal slices of 8 mm thickness are acquired for each of the six to seven stacks.

Although we had a cohort of athletes in our study, this technique could be applied to obese patients with equal facility. To account for greater body mass, the slice thickness can be increased, which slightly reduces the specificity of the technique, or the number of slices can be increased, which slightly increases the time of acquisition. All MRI tables have tabletop weight restrictions (usually 300–350 lb) and limited bore size (60 × 60 cm on the Intera). These restrictions preclude analysis of extremely large

patients on the system we used. However, the offline analysis program we have developed could be applied to data from any MRI machine, and because it realigns information according to information obtained in the DICOM header, whole-body analysis could be applied even without a moving tabletop, as long as meticulous patient positioning was observed. Hence, the imaging units that are currently used to image the largest patients in clinical practice today could be adapted to measure body fat content with this software.

In conclusion, we have developed a technique that, by combining MRI and CAD, makes it possible to improve the ease, efficiency, and effectiveness with which the analysis of body fat distribution can be conducted on a routine basis.

TABLE 1: Estimated Body Mass Index, Calculated Body Mass Index, and Derived Body Fat Detected

Male Subjects	Age	Measured BMI	Calculated BMI	Calculated % Body Fat	Female Subjects	Age	Measured BMI	Calculated BMI	Calculated % Body Fat
1	31	32.6	28.67	29.45	1	27	19.3	18.11	21.06
2	33	24.1	23.54	17.27	2	29	24.8	23.53	30.54
3	32	25.4	23.73	27.79	3	20	20.3	19.72	19.61
4	51	27.3	24.43	16.85	4	53	26.8	24.07	34.36
5	29	25.0	22.76	17.36	5	56	22.5	20.77	28.66
6	29	24.8	22.59	6.97	6	27	20.8	20.23	25.21
7	29	25.0	23.68	13.06	7	21	24.6	21.73	30.29
8	28	21.6	19.58	4.77	8	43	21.9	20.59	29.02
9	49	31.1	28.42	30.07	9	41	25.6	26.69	37.46
10	52	34.7	32.58	25.98	10	19	18.0	17.68	15.89
11	24	28.7	23.18	6.24	11	26	21.8	22.21	16.39
12	28	28.7	26.91	31.79	12	18	25.3	26.83	28.89
13	23	26.3	22.62	10.32	13	26	30.5	30.96	38.05
14	19	21.5	19.63	11.63	14	33	22.8	24.11	17.99
15	28	26.3	25.58	20.04	15	23	20.5	22.10	23.71
16	25	18.9	22.30	11.57	16	25	20.3	20.89	19.97
17	26	26.9	24.80	12.21	17	25	29.4	30.74	41.67
18	24	20.9	21.12	6.24	18	27	25.7	25.86	31.78
19	26	27.7	27.58	21.19	19	55	25.1	28.52	35.20
20	30	26.0	25.20	14.96	20	53	20.8	24.27	29.66
21	45	29.9	32.70	28.3	21	42	23.7	23.65	25.16

Note—BMI = body mass index.

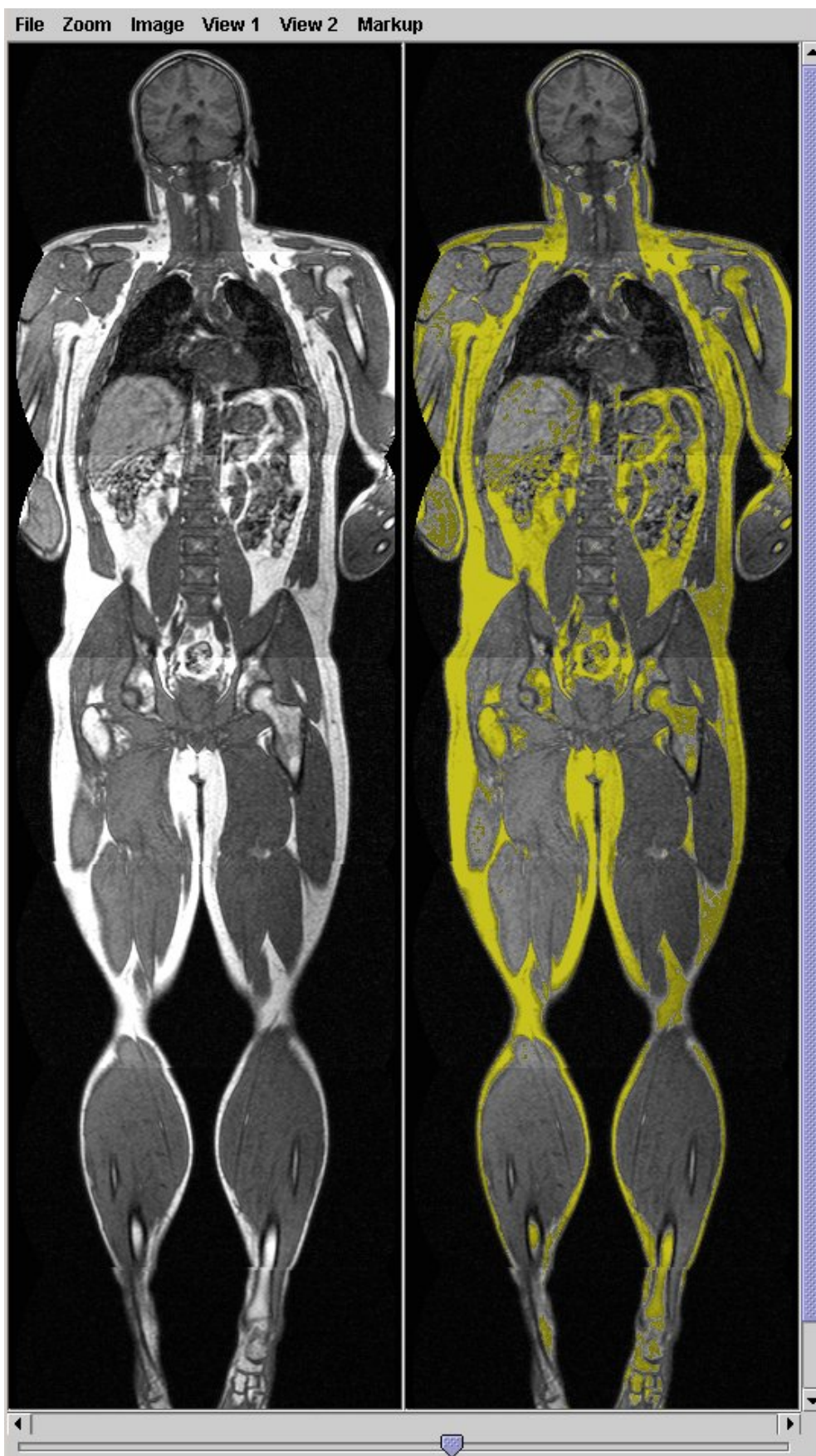


Fig 1. 28-year-old female volunteer. System display output illustrating localized regions identified as fat (marked in yellow in image on right). Slider bar allows user to step through image sequence. Image on left is original data after alignment and basic image processing to reduce noise artifacts

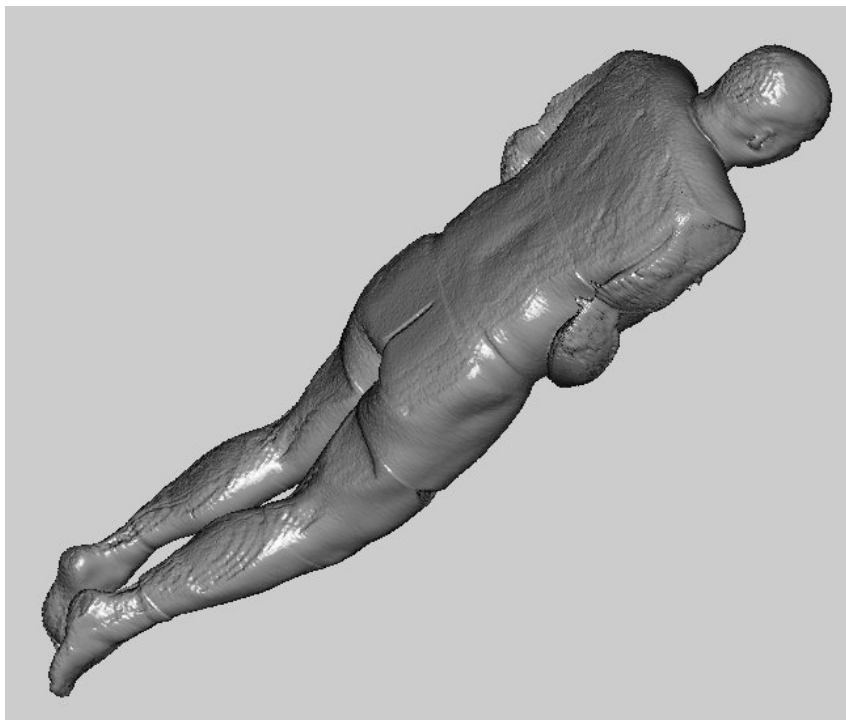


Fig 2. - 28-year-old female volunteer. Volume rendering of full-body MRI data set giving overview of patient's superficial body-fat distribution. This fully interactive 3D model allows flexible data clipping to be performed, which enables detailed analysis of regional fat distribution

Series #1: 250 x 32 x 937, 2.022059mm x 8.0mm x 2.022059mm
Name:
Weight: 90.0kg
Sex: M
Date of birth: 20/10/1972

Estimated full body volume = 98,422.84cc
Estimated full body height = 1.89m

Calculated Body Fat Table:-

	Method 1	Method 2
Body weight DICOM	90kg	90kg
Body weight calculated	103.14kg	102.91kg
Estimated BMI	28.73	28.67
Fat by volume	31,803.91cc	33,016.37cc
Fat by weight	29.2kg	30.31kg
% by volume	32.31%	33.55%
% by DICOM weight	32.44%	33.68%
% by calculated weight	28.31%	29.45%

Fig 3.- —System output text on per patient basis in 31-year-old male volunteer. Two slightly different methods for fat calculation are used. DICOM weight is that entered by the MRI technologist and is inaccurate in this patient, whose body weight was 102 kg. System provides accurate assessment of body fat. By applying clipping tool to 3D volume-rendered image (see Fig. 2), similar detailed voxel-by-voxel interrogation of particular body region can be performed.

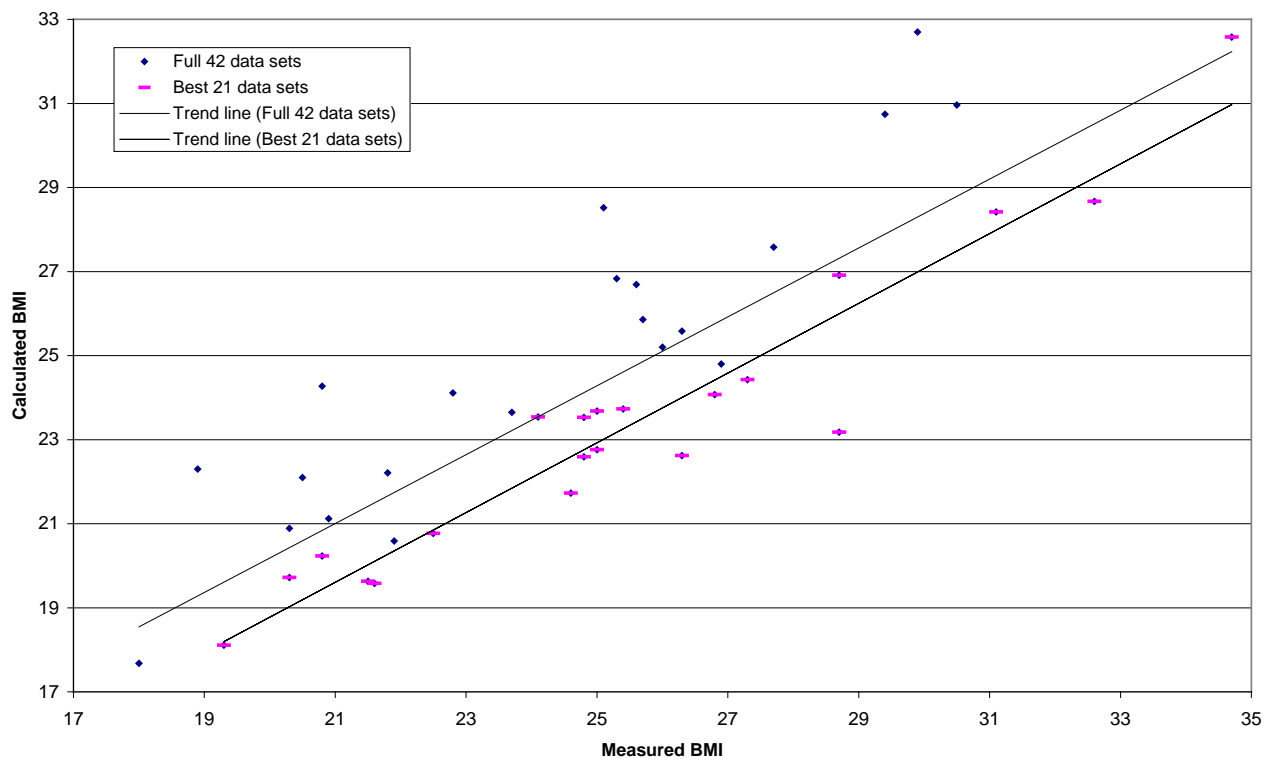


Fig 4.

Comparing manually measured BMI and the automatic CAD calculation. This illustrates that the CAD system does a good job in matching the manual BMI measurements. This test was used as an initial validation of the segmentation procedure and demonstrates that the CAD system developed produces reliable measurements. See the text for a full discussion.

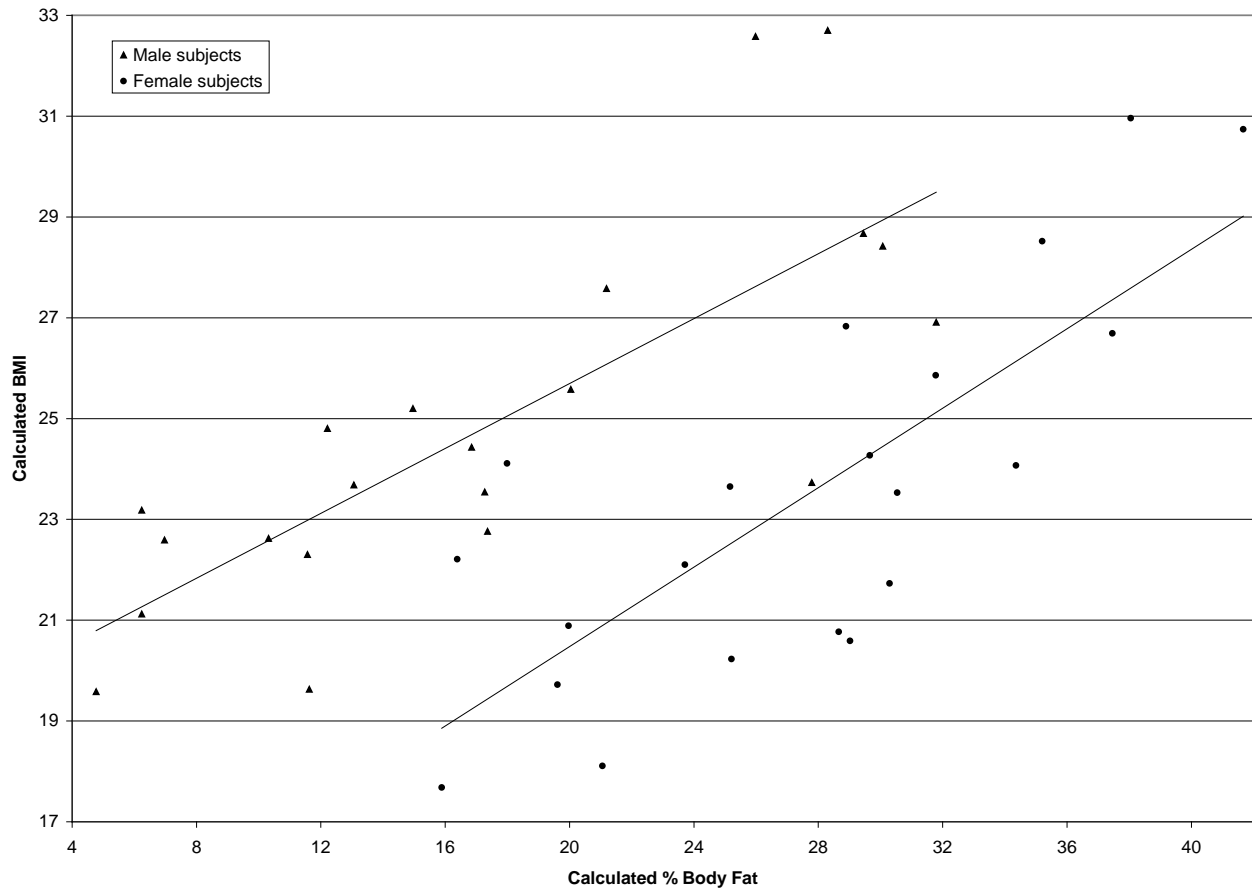


Fig 5.

BMI mapped against percentage body fat. The data is divided by gender and the two trend lines clearly illustrate the gender difference. Men tend to have a lower percentage body fat than women for the same BMI. The very lean subjects coming from the cohort of athletes examined further lift the trend line for the male subset, as their high muscle mass offsets low body fat and results in relatively high BMI values in this group, situated at the extreme left of the graphed data. The complexity of the relationship between percentage body fat and BMI illustrates the shortcomings of BMI as a reliable indicator of body fat.

References:

1. Kang Y, Engelke K, Kalender WA. A new accurate and precise 3-D segmentation method for skeletal structures in volumetric CT data. *IEEE Trans Med Imaging* 2003; 22:586–598
2. Nord RH, Payne RK. Body composition by dual-energy X-ray absorptiometry: a review of the technology. *Asia Pac J Clin Nutr* 1995; 4:173–175
3. Seidell JC, Bakx JC, De Boer E, Deurenberg P, Hautvast JG. Fat distribution of overweight persons in relation to morbidity and subjective health. *Int J Obes* 1985; 9:363–374
4. Seidell JC, Hautvast JG, Deurenberg P. Overweight: fat distribution and health risks. Epidemiological observations. A review. *Infusionstherapie* 1989; 16:276–281
5. Abu-Abid S, Szold A, Klausner J. Obesity and cancer. *J Med* 2002; 33:73–86
6. Onyike CU, Crum RM, Lee HB, Lyketsos CG, Eaton WW. Is obesity associated with major depression? Results from the Third National Health and Nutrition Examination Survey. *Am J Epidemiol* 2003; 158:1139–1147
7. Speranza M, Corcos M, Atger F, Paterniti S, Jeammet P. Binge eating behaviours, depression and weight control strategies. *Eat Weight Disord* 2003; 8:201–206
8. Dixon JB, Dixon ME, O'Brien PE. Depression in association with severe obesity: changes with weight loss. *Arch Intern Med* 2003; 163:2058–2065
9. Deurenberg P, Pieters JJ, Hautvast JG. The assessment of the body fat percentage by skinfold thickness measurements in childhood and young adolescence. *Br J Nutr* 1990; 63:293–303
10. Deurenberg P, Deurenberg-Yap M. Validation of skinfold thickness and hand-held impedance measurements for estimation of body fat percentage among Singaporean Chinese, Malay and Indian subjects. *Asia Pac J Clin Nutr* 2002; 11:1–7
11. Widhalm K, Schonegger K, Huemer C, Auterith A. Does the BMI reflect body fat in obese children and adolescents? A study using the TOBEC method. *Int J Obes Relat Metab Disord* 2001; 25:279–285
12. Deurenberg P, Deurenberg-Yap M, Guricci S. Asians are different from Caucasians and from each other in their body mass index/body fat percent relationship. *Obes Rev* 2002; 3: 141–146
13. De Lorenzo A, Deurenberg P, Pietrantuono M, Di Daniele N, Cervelli V, Andreoli A. How fat is obese? *Acta Diabetol* 2003; 40 [suppl 1]:S254–S257
14. Prentice AM, Jebb SA. Beyond body mass index. *Obes Rev* 2001; 2:141–147
15. van der Kooy K, Leenen R, Seidell JC, Deurenberg P, Droop A, Bakker CJ. Waist-hip ratio is a poor predictor of changes in visceral fat. *Am J Clin Nutr* 1993; 57:327–333
16. Bedogni G, Pietrobelli A, Heymsfield SB, et al. Is body mass index a measure of adiposity in elderly women? *Obes Res* 2001; 9:17–20
17. Vescovi JD, Hildebrandt L, Miller W, Hammer R, Spiller A. Evaluation of the BOD POD for estimating percent fat in female college athletes. *J Strength Cond Res* 2002; 16:599–605
18. Fogelholm M, van Marken Lichtenbelt W. Comparison of body composition methods: a literature analysis. *Eur J Clin Nutr* 1997; 51:495–503
19. McNeill G, Fowler PA, Maughan RJ, et al. Body fat in lean and overweight women estimated by six methods. *Br J Nutr* 1991; 65:95–103
20. Mazess RB. Accuracy of TOBEC method questioned. *Am J Clin Nutr* 1984; 39:157–159
21. Robin JP, Heitz A, Le Maho Y, Lignon J. Physical limitations of the TOBEC method: accuracy and long-term stability. *Physiol Behav* 2002; 75:105–118
22. Seidell JC, Oosterlee A, Deurenberg P, Hautvast JG, Ruijs JH. Abdominal fat depots measured with computed tomography: effects of degree of obesity, sex, and age. *Eur J Clin Nutr* 1988; 42:805–815
23. Seidell JC, Oosterlee A, Thijssen MA, et al. Assessment of intra-abdominal and subcutaneous abdominal fat: relation between anthropometry and computed tomography. *Am J Clin Nutr* 1987; 45:7–13
24. Sjostrom L. A computer-tomography based multicompartiment body composition technique and anthropometric predictions of lean body mass, total and subcutaneous adipose tissue. *Int. J Obes* 1991; [suppl 2]:19S–30S

25. Abate N, Burns D, Peshock RM, Garg A, Grundy SM. Estimation of adipose tissue mass by magnetic resonance imaging: validation against dissection in human cadavers. *J Lipid Res* 1994; 35:1490–1496
26. Fowler PA, Fuller MF, Glasbey CA, Cameron GG, Foster MA. Validation of the in vivo measurement of adipose tissue by magnetic resonance imaging of lean and obese pigs. *Am J Clin Nutr* 1992; 56:7–13
27. Fowler PA, Fuller MF, Glasbey CA, et al. Total and subcutaneous adipose tissue in women: the measurement of distribution and accurate prediction of quantity by using magnetic resonance imaging. *Am J Clin Nutr* 1991; 54:18–25
28. Kamel EG, McNeill G, Han TS, et al. Measurement of abdominal fat by magnetic resonance imaging, dual-energy X-ray absorptiometry and anthropometry in nonobese men and women. *Int J Obes Relat Metab Disord* 1999; 23:686–692
29. Thomas EL, Saeed N, Hajnal JV, et al. Magnetic resonance imaging of total body fat. *J Appl Physiol* 1998; 85:1778–1785
30. Abate N, Garg A, Coleman R, Grundy SM, Peshock RM. Prediction of total subcutaneous abdominal, intraperitoneal, and retroperitoneal adipose tissue masses in men by a single axial magnetic resonance imaging slice. *Am J Clin Nutr* 1997; 65:403–408
31. Thomas LW. The chemical composition of adipose tissue of man and mice. *Q J Exp Physiol Cogn Med Sci* 1962; 47:179–188